Research Article

International Journal of Advanced Technology and Engineering Exploration, Vol 11(121)
ISSN (Print): 2394-5443 ISSN (Online): 2394-7454
http://dx.doi.org/10.19101/IJATEE.2024.111100140

Automated liver image segmentation using entropy-based thresholding and median filtering

Sangeeta K Siri[1], Sudha M S[2], Baby H T[3], Pramod Kumar S[4*], Pradeepa S C[4] and Abhijith N[4]
Global Academy of Technology, Bengaluru, Karnataka, India-560098[1]
Cambridge Institute of Technology, Bengaluru, Karnataka, India-560036[2]
Government Engineering College, Mosalehosahalli, Karnataka, India-573212[3]
JNN College of Engineering, Shivamoga, Karnataka, India-577204[4]

Received: 07-February-2024; Revised: 23-December-2024; Accepted: 24-December-2024

Abstract
The separation of liver images from abdominal scans has emerged as a critical focus in biomedical image processing, serving as a foundational step in automated techniques for liver disease diagnosis, treatment planning, and follow-up assessment. Current medical research and case studies underscore the challenges of liver segmentation, primarily due to the low contrast between the liver and surrounding tissues in computed tomography (CT) images. Furthermore, the liver's edges are often indistinct, and its texture, shape, color, and size exhibit significant variability. With advancements in medical imaging technology, the volume of data requiring processing has grown substantially, highlighting the need for automated methods to replace time-intensive manual segmentation procedures. In response to these challenges, a novel threshold-based segmentation technique has been introduced, utilizing liver image entropy as a measure of information content. The process involves denoising with a median filter, followed by cropping a random section of the liver image to determine its entropy distribution. This distribution establishes upper and lower bounds, facilitating precise separation of the liver from its background. The proposed method was evaluated on CT scan images from 60 patients, addressing diverse and complex segmentation scenarios. Key performance metrics, including maximum edge distance (MED), relative volume difference (RVD), accuracy, and dice similarity factor (DSF), were employed to benchmark the model against expert-traced reference images. The results indicate an average MED of 12.5 mm, an average RVD of 4.2%, an average accuracy of 91.70%, and an average DSF of 90.95%. These results demonstrate the effectiveness of the proposed model as a robust tool for computer-aided decision support systems, significantly advancing the accuracy and reliability of clinical diagnosis.

Keywords
Liver segmentation, Computed tomography, Entropy-based thresholding, Automated image processing, Medical imaging, Computer-aided diagnosis.

1.Introduction
The liver is the biggest gland and largest internal organ. Thus, it performs dual roles in the human body. It is a vital and unique organ without which the tissues of the body speedily perish from deficiency in vitality and nutrients. At the same time, the liver has a limited ability to regenerate dead or damaged tissues. Hence, no mechanism or medicine can compensate for the loss of liver functions. It is a reddish-brown organ with lobes of irregular size and shape. The liver's size is dependent on numerous factors: age, gender, body size, weight, and health conditions [1]. It is situated in the right section of the abdominal cavity just below the diaphragm and some part extends towards the left [2].

The gallbladder is located under the liver along with sections of the pancreas, kidneys and intestine. The liver is essential for detoxification, immunity, digestion, metabolism, vitamin storage, and other vital functions. Due to its large blood flow, location in the body, and anatomy, it is more prone to various diseases. There are more than 100 disorders of the liver, which may be due to toxins, viruses, alcohol, genetics, imbalanced food intake, obesity, poor sanitary habits, drugs, and other factors [3]. The most widespread diseases are liver cancer, alcoholic

*Author for correspondence

hepatitis, fatty liver, viral hepatitis, cirrhosis, fulminant hepatic failure [4], and others. Primary liver cancer is the sixth most common cancer in the world and the fourth leading cause of death from liver failure [5, 6]. Several medical imaging modalities are available today, including magnetic resonance imaging (MRI), computed tomography (CT), ultrasound, digital mammography, and angiography. These modalities significantly enhance the identification of healthy and diseased anatomy for accurate diagnosis and effective treatment planning. Among these, radiologists often prefer CT scans due to their superior spatial resolution, higher signal-to-noise ratio, and greater anatomical accuracy [7].

Owing to significant advancements in medical imaging modalities, managing large volumes of data requires computational support. Radiological tasks may be made easier with the use of liver image segmentation algorithms for the delineation of the liver from an abdominal CT scan. Furthermore, liver segmentation algorithms are essential for tasks like detecting pathology, disease progression, quantification of liver volume, and monitoring treatment response. Liver segmentation also helps in identifying significant indices in cases of living donor liver transplantation [8], initiating radiation treatment procedure [9], surgical planning prior to hepatectomy [10] and depiction of the liver volume in three dimensions(3D) [11]. Hence, extracting the liver area from the CT scan is a crucial issue that is addressed by many researchers. The liver parenchyma is often manually outlined on each CT slice by experts, which is quite time-consuming. The development of automated and semi-automated procedures has received increased attention, with numerous articles published on the subject [4].

Liver segmentation is essential and it is a very challenging task because of its anatomical structure each patient has a different pixel intensity, and this intensity varies throughout the liver [12, 13]. This might be due to the hereditary factors or diseases associated with the patient. Hence, region-based and clustering segmentation algorithms fail to provide an accurate liver image [14]. The edge-based segmentation algorithms allow for delineation of the precise liver border, even though the edges are hazy [15]. The liver pixel intensity range has proximity to its neighboring organs like gall bladder, stomach, kidney, etc.; hence finding thresholds to separate the liver from its neighboring organs is a difficult task. General imaging and motion artifacts also affect the functioning of liver segmentation algorithms [16]. Additionally, each imaging modality has its own specific challenges, which must be handled by the liver segmentation algorithm. Currently, there is no single, segmentation algorithm that offers reasonably acceptable results for different modalities such as positron emission tomography (PET), MRI, CT, etc. [17]. Due to the importance and necessityof liver segmentation, it has become an active research area [18]. Several novel and exciting perspectives, that have developed in the last four decades shed light on this complex research area. Nowadays, regression-based, clustering-based, and deep learning-based methods are innovative and trendy techniques [19].

The significance of liver segmentation in the medical field and challenges in separating liver from abdominal CT scan images motivated us to develop a fully automatic liver segmentation model. The first objective of the proposed work is to design a fully automatic liver segmentation framework based on the entropy of the liver image. The second objective of the proposed model is to design and analyse a fully automatic segmentation framework that offers accurate and consistent results. The third objective is to compare the proposed model with state-of-the-art techniques and reference images obtained from an expert operator using evaluation metrics.

The key contributions of our framework are as follows:

1. Development of a image entropy-based liver segmentation technique, which can serve as a biomarker for computer-aided disease (CAD) diagnosis schemes.
2. Implementation and experimentation using MATLAB 2019a version.
3. Comparison of the proposed model with conventional entropic segmentation, demonstrating superior performance.
4. Evaluation of the proposed model using key metrics, including maximum edge distance (MED), relative volume difference (RVD), accuracy, and dice similarity factor (DSF).

The paper is organized into six sections. Section 1 introduces the proposed work, including the background, challenges, necessity of liver segmentation, motivation for the proposed model, and objectives. Section 2 presents a survey of previous work in the field of fully automatic liver segmentation. In Section 3, the fully automatic liver segmentation framework is described in detail. Section 4 discusses the experimental results of the proposed framework, while Section 5 focuses on the analysis of these results. Finally, the paper is concluded in Section 6.

2.Literature review

In this section, the related work is discussed, highlighting the advantages and challenges that emphasize the need for this study. It explores the current status of the field and provides a summary of the existing body of knowledge.

Lu et al. [20] have utilized graph cut method to separate liver. In their framework, an initial coarse liver image is obtained using multi–atlas segmentation method. The accurate liver image is obtained using shape and multi-dimensional features with 94% of average volume overlap. The framework provides accurate results. The dataset used does not include acute liver diseases, making the results unsuitable for clinical purposes.

Nayantara et al. [21] proposed a deep learning framework in combination with leaky rectified linear unit (ReLU) layers and a segmented neural network (SegNet)to extract an intact liver image from CT scan dataset. This framework achieves a DSF of 96%. The dataset is large and covers all kinds of liver diseases and provides precise results for liver delineation, but it is sensitive to CT image format.

Ahmed et al. [22] developed a new convolutional-neural network (CNN) for liver delineation. They have utilized 3 convolution layers; every layer is tracked by max-pooling layer. Finally, a two-way softmax function is used. Random Gaussian initialization is used to provide initial weights. The framework is tested on Sliver07 dataset providing DSF, Jaccard Coefficient (JC), specificity, accuracy and sensitivity as 0.95, 0.91, 0.99, 0.97 and 0.97 respectively. The outcomes are promising for clinical applications, but a large dataset is necessary to train the CNN model, which can be time-consuming and expensive.

Siri et al. [23] have utilized “slope difference distribution (SDD)” of image histogram to detach liver image in CT scans. The framework employs a median filter to reduce noise and SDD to produce thresholds that correctly separate the liver portion from CT images with JC of 91%. This model provides best results compare to the state-of-art but struggles to accurately segment the liver image in cases involving acute diseases. Siri et al. [24] introduced neutrosophic set (NS) to separate the liver image from CT images. In this study, the abdominal CT scan is converted into NS, which is divided into three subsets: edge, non-object, and object. The hepatic region is specified by the object subset. To obtain an accurate liver image from abdominal CT scan, morphological operations are carried out on a subset of the objects, which delivers an average positive rate of 92%. The model offers the best results; hence it can be used for clinical purpose. The limitation of the model is that its results depend entirely on the accuracy of liver section cropping.

Zhang et al. [25] developed a novel deep learning model which extracts circular regions to detect hepatic steatosis to obtain exact liver image from abdominal CT scan with 95% confidence interval. The anticipated novel model offers accurate liver delineation from CT scans considering moderate to severe hepatic diseases but requires a large dataset for training, which is both time-consuming and resource-intensive.

Alirr [26] utilize a fully convolutional neural network (FCN) combined with a localized region-based level set method to distinguish between liver tissue and tumors in CT scan images. In this method, the model is trained to segregate coarse liver and malignancy using FCN. Localized region-based level techniques applied to a research institute against digestive cancer (IRCAD) dataset, achieving DSF of 95.2% and 76.1% for the liver and its tumor segmentation, respectively. This model has demonstrated its capability for robustness and be promising tool for analysis of liver and its tumours in the clinical routine but requires more time for liver and tumour detection.

Rehman et al. [27] designed liver and tumor segmentation using hybrid residual U-Net (ResUNet) model, which is a blend of U-Net and residual network (ResNet)models. The model is experimented on public 3-dimensional dataset of IRCAD. This framework of liver segmentation offers liver segmentation accuracy of 99.6% and tumor classification rate of 98%. The model delivers admirable results in terms of diagnosing quickly and proficiently, but requires a bigger dataset for training.

Napte et al. [28] introduced a CNN with an encoder-decoder model, experimented on the liver tumor segmentation benchmark (LiTS) dataset, achieving a DSF of 0.96 and JC of 0.92, respectively. This model employs Kirsch’s filter to boost edge and texture information of liver area. This model reduces over segmentation and under- segmentations, thereby increasing Acc. The disadvantage of the recommended framework is its greater complexity, a large number of trainable parameters, and longer training time due to the use of two parallel U-Nets.

Lou et al. [29] separate liver image in CT scan images using Shannon entropy. The dilation and erosion are employed to obtain exact liver image, providing satisfactory results with DSF of 95.12%. Extensive tests confirm the efficacy of the proposed method. This model is ineffective in the presence of significant noise.

Gao et al. [30] introduced a V-Net model for coarse segmentation and a hybrid level set method for accurate segmentation. This model achieves a notable precision of 95.13% in liver segmentation. The results were tested on large datasets, confirming the efficiency of the framework, which improved the accuracy. However, the framework requires a large dataset for training, which can be time-consuming and expensive.

Ozcan et al. [31] designed combined approach using an inception model and CNN-based U-net which delineate both liver and its tumor with average accuracy of 99.75% on LiTS dataset. This framework is a hundred times faster than manual segmentation; however, it increases the burden on the graphics processing unit (GPU) and training time.

Ayalew et al. [32] introduced a novel U-Net-based model that uses a smaller number of filters, along with more dropout layers and batch normalization. The outcomes demonstrate accuracy of 0.99 on the LiTS dataset. The algorithm achieves a DSF of 0.96 for liver segmentation but faces challenges with separating small tumors in the liver. Khoshkhabar et al. [33] proposed a new deep learning-based technique to extract the liver and its tumor from CT scan images. This framework integrates a fully connected layer and four Chebyshev graph convolution layers. The proposed method achieves a DSF of 91.1% and an accuracy of 99.1% when tested on the LiTS17 database. The model achieves high accuracy in noisy environments. The major drawback of this model is that experimentation was not performed on a real-time dataset.

Balakrishnan et al. [34] proposed an advanced liver segmentation technique based on the M-Net approach. Noise is removed using wavelet transform and bilateral filter. The features are extracted using a Gabor filter. For classification, the best feature subset is selected using the hybrid genetic algorithm (HGA). Subsequently, the ensemble deep CNN method is employed for the classification process. The accuracy obtained using this framework is 0.89. The accuracy of classification is high for varied dataset, but the system is complex.

Giri et al. [35] developed an efficient liver segmentation algorithm that isolates liver from 3D-CT scan images. The model begins with improving CT image quality through voxel resampling and intensity normalization. Skip connections and an encoder-decoder network are employed to collect both local and global contextual data for U-Net models. Linked component analysis is performed to remove false positive results. This framework achieves dice score (DC) of 0.93. This model shows a similarity between the predicted and reference images although taking more time for training.

Uplaonkar et al. [36] proposed liver tumor segmentation from ultrasound images. The image quality is improved using the adaptive histogram equalization technique. Subsequently, liver tumors are segmented through the combined efforts of Otsu threshold-based level set and local bidirectional ternary pattern. The model achieves a segmentation accuracy of 99.43%. The model provides fast results with high Acc, but it is sensitive to noise. Cao et al. [37] designed an automatic kidney segmentation network based on deep learning models. It integrates the decoding module and multi-scale spatial perception module. This achieves a precision of 98.52%. The system is more robust to variations in renal sizes, shapes, and imaging setting compared to manual techniques, as it learns patterns from a large dataset. The performance of the model is extremely dependent on the quality and variety of the training datasets.

Ouyang et al. [38] proposed an innovative liver segmentation model using CT scan images based on SwinNet, which utilizes swin transformer block and skip connections. This attains high accuracy and reduces computational complexity. This model offers DSF of 0.9730 and intersection of union (IoU) of 0.9541. Removal of skip connections in the initial layers helps reduce computational costs, but it could hypothetically limit the network's ability to retain low-level feature details, which could influence segmentation efficacy in some cases. Biswas et al. [39] focused their work on improving the training efficacy of conventional segmentation schemes using generative adversarial network (GAN). This method generates more high-quality training samples.

Subsequently, a geometric active contour model is utilized to extract liver segmentation, achieving a DSF of 0.872 on LiTS.The inclusion of GAN-generated images in the pre-segmentation phase allows for competent preliminary tumour localization, making it easier for subsequent segmentation to improve the contours and regions of interest. Training GANs can be computationally expensive and time-consuming.

A review of the literature on image segmentation techniques reveals a wide range of innovations and approaches that support several applications in domains including computer vision, autonomous driving, and medical imaging. Techniques for segmenting images may be roughly divided into three groups: conventional methods such as deep learning-based algorithms, conventional methods (like thresholding, clustering, edge detection, etc.) and hybrid models. Each group has advantages and disadvantages based on the particular use and type of image.

Image segmentation has seen a substantial transformation with the introduction of deep learning, since the CNN are now attaining state-of-the-art performance. New standards in segmentation tasks have been set by architectures such as U-Net and SegNet, especially in complex environments like medical imaging. Recent developments point toward hybrid models that blend classical techniques with deep learning methods, exploiting their respective strengths to improve segmentation accuracy and robustness. Despite these advances, issues remain, such as coping with noise, occlusions, and differences in lighting and size. Additionally, the computational demands of deep learning algorithms and the requirement for large annotated datasets are major challenges researchers are addressing.

Recent developments indicate a shift toward hybrid models that combine classical techniques with deep learning methods, leveraging their respective strengths to enhance segmentation accuracy and robustness. However, challenges persist, including dealing with noise, occlusions, and variations in lighting and size. Furthermore, the high computational demands of deep learning algorithms and the need for large annotated datasets remain significant obstacles for researchers to overcome.

3.Methodology

Claude Shannon, in 1948, introduced the theory of information in his work titled "A Mathematical Theory of Communication" [40, 41]. This theory defined entropy as the average level of information or uncertainty inherent in the possible outcomes of a set of variables [42]. Specified a distinct random variables V, with probable outcomes $v_1, v_2, v_3 \ldots\ldots v_n$ which occurs with probability of $P(v_1)$, $P(v_2)$, $P(v_3)$ $\ldots\ldots P(v_n)$, that satisfies the condition $P(v_i)>=0$, where $\sum_{i=1}^{n} P(v_i) = 1$ and n=1, 2……

Shannon's entropy of V is defined as in Equation 1.

$$E(V) = -\sum_{i=1}^{i=n} P(v_i) \times log\, P\,(v_i) \quad (1)$$

Where ∑ indicates the summation over the variable possible values and log is logarithm, the selection of base varies depending upon applications. The base '10' gives a unit of "dits", while base of 'e' offers the "natural unit" "nat" and base '2' provides the unit of "bits". The amount of ambiguity of distribution V is called the entropy distribution of V which is denoted by E(V).

In image, entropy can be stated as corresponding states of intensity levels which individual pixel can adapt [43]. It is used in the quantitative exploration and estimation of image details. Entropy value is significant because it offers image details. In image processing, entropy is a statistical indicator of unpredictability that may be used to show how the input image's texture is composed [44]. The grey scale image's entropy is defined as in Equation 2.

$$E(I) = \sum_{i=0}^{i=255} (p_i \times log\,2\,(p_i)) \quad (2)$$

where, *p* contains the normalized histogram. Where normalized histogram is defined as in Equation 3.

$$\mathrm{Histo.norm} = [\mathrm{p}\ (\mathrm{x}, \mathrm{y}) - \mathrm{min.pixel\ value}] / [\mathrm{max.pixel\ value} - \mathrm{min.pixel\ value}] \quad (3)$$

where P (x, y) stands for pixel intensity value at (x, y). The pixel matrix forms an image which contains certain information. The information contents in an image are quantified by entropy [45]. Shannon's entropy is often referred as tool to assess the level of information that is present in a set of data (image), being greater when there is more information present, and zero when there is no information present in the set of data (image) [46].

Exploiting the concept of Shannon's entropy, the following steps are designed to extract liver image from CT scan image precisely.

Step 1: Read the CT scan image. The CT scan is in color format with 1024×800. In order to reduce computational cost, it is converted into gray scale and resize to 256×256.

Step 2: Use median filter of 3×3 which removes noise in an image whilst perpetuate sharp features. The choice of a 3×3 median filter is deliberate due to its well-known capability in reducing impulsive noise (such as salt-and-pepper noise) while preserving important edge features in the image. This is critical in medical image processing, where maintaining the integrity of anatomical boundaries, such as the liver, is essential for accurate segmentation. A 3×3 filter size is specifically chosen as it provides a balance between noise reduction and computational efficiency, ensuring that image quality is retained without excessive smoothing of crucial structures.

Step 3: Crop random section of liver.

Step 4: Histogram of cropped liver is normalized using Equation 3.

Step 5: Divide the entropy distribution of cropped liver section into two sub-ranges: (1) Foreground /object distribution and (2) Background distribution. The liver is largest internal organ places at right abdominal section of human body. Along with this, pixel intensity values vary from patient to patient as well as one section of liver to other section of liver which may be due to inherent property, pathology, etc. So, entropy of liver varies which is shown in *Figure 1*. The lower bound and upper bound provide the variation in liver pixel intensity. Using these bounds, the liver image can be separated from abdominal CT scan images. *Figure 1* shows foreground entropy-distribution of cropped liver section. In this, liver entropy varies from pixel level 145 to 208. From pixel level 209 to 256, entropy is constant. So lower bound-145 and upper bound = 208. Using lower bound and upper bound delineate liver image from its background since liver image lies between upper and lower bound. The entropy distribution of liver shows that the pixel values ranging between 0 to 144 are absent in liver image i.e. these pixel values correspond to background. In an image, entropy can be stated as corresponding states of intensity levels which individual pixel can adapt [40]. It is used in the quantitative exploration and estimation of image details. Entropy value is significant because it offers image details. To address this variability, a double-threshold method was employed. Specifically, a lower bound and an upper bound for pixel intensities were determined to capture the range of liver intensity values. These threshold values allow for accurate segmentation of the liver from the surrounding abdominal structures in CT scan images. The method effectively isolates the liver by excluding pixels outside this defined range.

Step 6: From Equation 4, the randomness or variation of the foreground (liver) is achieved. In other words, entropy distribution of foreground provides upper bound and lower bound for double- threshold method (as shown in *Figure 1*).

Step 7: Apply double-threshold method to delineate the liver image from its surrounding organs and tissues as follows in Equation 4.

$$I_{thresh} = \left\{ \begin{array}{ll} P(x,y) & if\ lower\ bound < I < upper\ bound \\ 0 & Otherwise \end{array} \right\} \quad (4)$$

Step 8: Morphological operations are applied to obtain a clearer liver image and define its periphery. Erosion is performed first to eliminate small, unwanted pixel clusters at the liver image's edges. This is followed by dilation, which enhances the visibility of the liver and fills any small holes that may be present. *Figure 2* illustrates the flowchart of the proposed model.

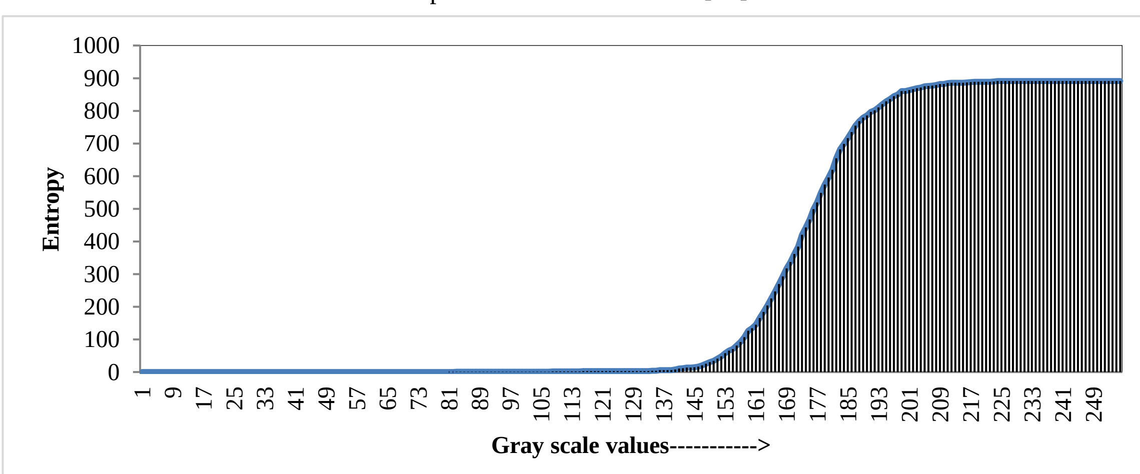

Figure 1 Foreground entropy-distribution of cropped liver section

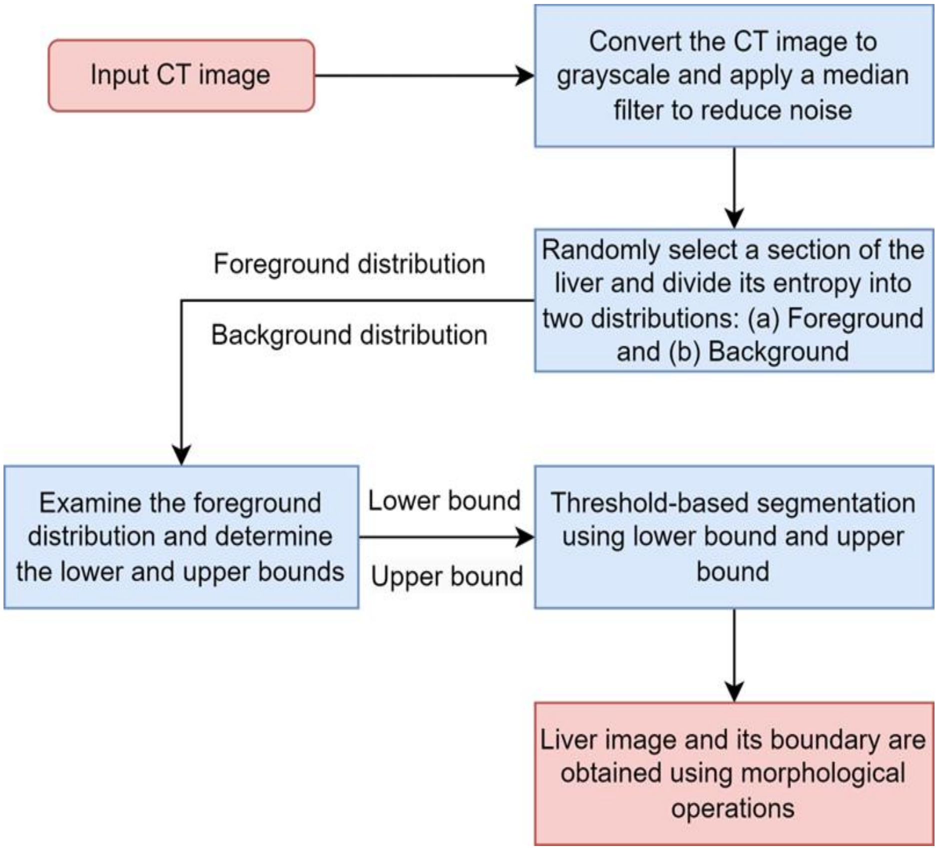

Figure 2 Flowchart of entropic liver segmentation

4.Results

The test dataset comprises CT scans of 60 different patients which are collected from CT scan Centre, LG F, Eureka Junction, 6-13, Travellers Bunglow Rd, Deshpande Nagar, Hubballi, Karnataka 580029, India. The CT slices are 1019×682 color images. The number of slices in each case ranged from 40 to 550. The pixel spacing varied from 0.56 to 0.84 mm, and the slice thickness from 1 to 4 millimetre. The dataset includes both healthy and diseased liver cases to ensure a robust and generalized framework for segmentation and analysis. This diversity in the dataset is crucial for developing a method that can effectively handle various liver pathologies, thus enhancing the reliability and applicability of the segmentation approach. The proposed entropic segmentation has been implemented in MATLAB-R2019a version. It runs on Windows 10 OS, with an Intel i5-3210M processor.

Entropy has an extensive range of applications in the field of image processing, such as noise removal and image enhancement. The concept of entropy is applied to determine accurate double threshold values (upper bound and lower bound), which represent the liver pixel intensity range. The upper and lower bound separates the liver from its surrounding organs and tissues.

In the liver, there is wide variation in the pixel intensity range from one section of liver to another. Entropic segmentation yields highly effective results. *Figure 3* illustrates the details of the proposed framework: (a) the original CT scan image, (b) random cropping of the liver, (c) the result of entropy-based liver segmentation, (d) the final liver segmentation after post-processing, (e) the accurate liver border marking in CT images, and (f) the ground truth image.

Threshold-based liver segmentation is inherently the fastest, simplest, and the least mathematically complex. It is one of the oldest and most common methods to figure out an object from its background in image processing. This involves selecting grayscale values into subranges corresponding to the constituent regions of the image, subject to these regions being distinguishable based on brightness.

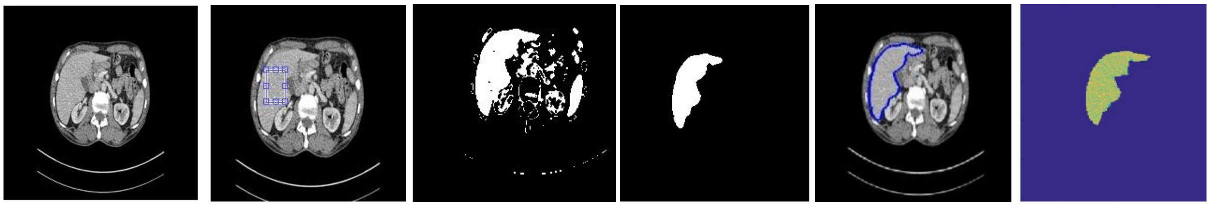

(a) (b) (c) (d) (e) (f)

Figure 3 Outcomes of proposed entropic segmentation model; (a) 2-D CT scan image; (b) output of median filter with random liver image cropped; (c) Entropy based thresholding output with lower bound=153 and upper bound=210 (obtained from entropy graph); (d) Final liver segmentation after post processing; (e) CT scan image with liver border; (f) Ground truth image

Threshold-based liver segmentation is inherently the fastest, simplest, and the least mathematically complex. It is one of the oldest and most common methods to figure out an object from its background in image processing. This involves selecting grayscale values into subranges corresponding to the constituent regions of the image, subject to these regions being distinguishable based on brightness.

4.1Quantitative analysis

Biomedical image segmentation has made significant strides in recent years. There are various distinct characteristics that define biomedical image segmentation. Therefore, evaluating the effectiveness of the segmentation method is crucial [47, 48]. The outcome of the segmentation technique is named SEGALG and ground truth image acquired with the help of expert is called as SEGGT. These two images are compared using segmentation evaluation metrics. This determines how similar or different they are to each other. RVD, MED, accuracy, and DSF are evaluation metrics utilized to assess the efficacy of the proposed framework.

4.1.1Relative volume difference (RVD)

The RVD between two sets, SEG_{ALG} and SEG_{GT}, is expressed as a percentage and defined in Equation 5, where SEG_{GT} represents the ground truth image, and SEG_{ALG} denotes the algorithm-segmented image [49]."

$$RVD = 100(|SEGALG - SEGGT|)/SEGGT \quad (5)$$

RVD of 0% indicates complete overlap between the two areas. The comparison between the proposed model and the threshold segmentation using the minimal cross-entropy segmentation method, along with the corresponding RVD values, is presented in *Figure 4.*

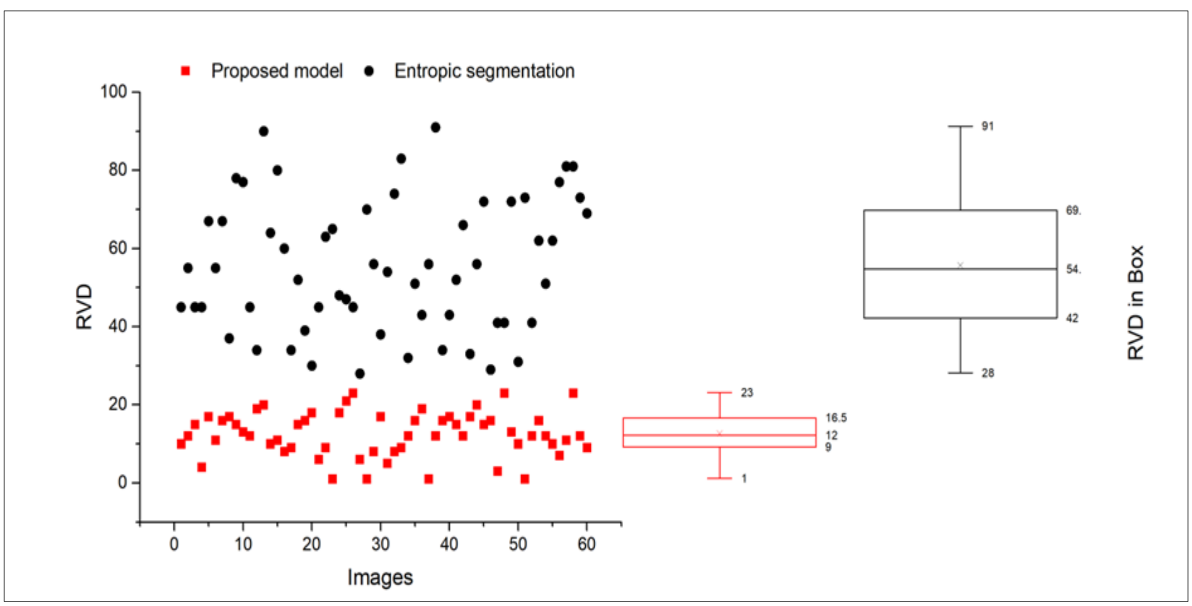

Figure 4 Evaluation of the proposed model against entropic approach using RVD

4.1.2Maximum edge distance (MED)

The Euclidean distance is calculated to retrieve maximum deviation of edge pixels of ground truth/reference liver image and algorithm segmented liver image. The unit of measurement is millimetre (mm) [50, 51]. For ideal segmentation, MED is 0 mm. It is shown in Equation 6.

$$MED = max[\,dist(SEG_{ALG}, SEG_{GT}), dist(SEG_{GT}, SEG_{ALG})] \quad (6)$$

Where SEG_{ALG} represents the liver edge pixels obtained from the algorithm, and SEG_{GT} represents the liver edge pixels obtained from the ground truth image. This parameter is sensitive to the liver's contour and highlights the maximum defect, which is a key requirement in surgical treatment. *Figure 5* presents a comparison between the proposed model and the state-of-the-art methods.

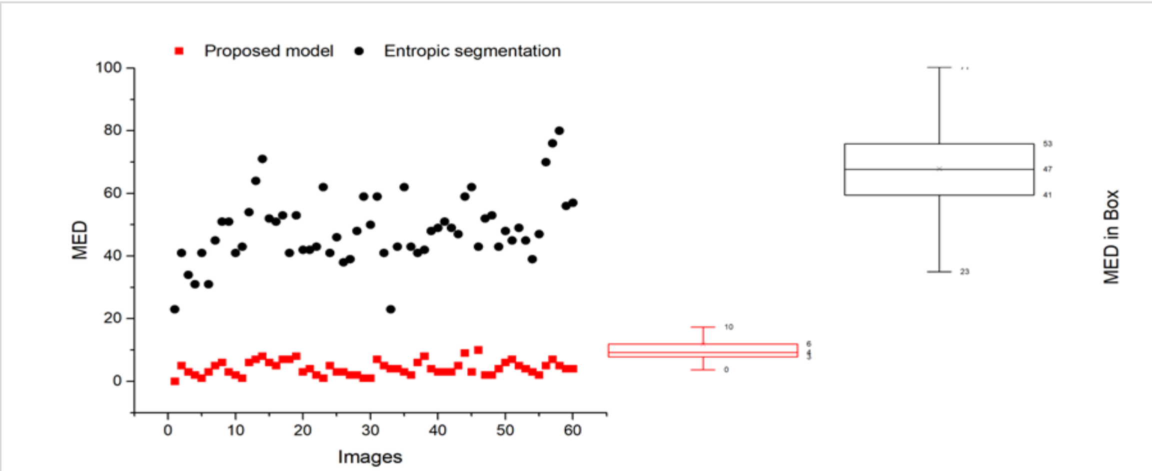

Figure 5 Assessment of the proposed model in comparison with entropic method using MED

4.1.3Accuracy

Segmentation accuracy analyses the deviation between ground truth image and segmentation predicted image. In this paper, the ground truth image is approved with the manual segmentation image under the supervision of a medical practitioner. The similarity between the ground truth image and the algorithm predicted image reflects the accuracy.

The accuracy measure is calculated as shown in Equation 7. The accuracy for liver segmentation using proposed model and state-of-the-art is shown in *Figure 6*. Accuracy is 1 if the segmentation is perfect, as defined in Equation 7. As accuracy moves away from one denotes deviation of segmentation.

$$Accuracy = \frac{Correctly\ predicted\ pixels}{Total\ number\ of\ pixels} \times 100 \quad (7)$$

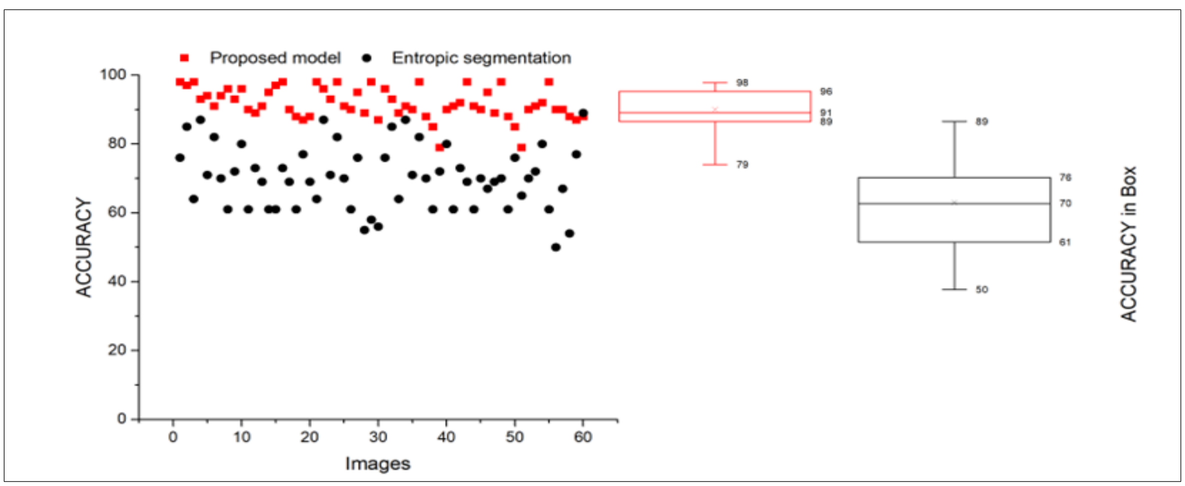

Figure 6 Accuracy comparison between the proposed model and entropic model

4.1.4Dice similarity factor (DSF)

The similarity of two objects is also evaluated by DSF. In this evaluation technique, dice's factor needs to be calculated to evaluate similarities [52]. DSF is defined in Equation 8.

$$DSF = 2 \times \frac{[SEG_{ALG} \cap SEG_{GT}]}{[SEG_{ALG} - SEG_{GT}]} \times 100 \quad (8)$$

where SEGALG and SEGGT are the segmented and ground truth, respectively. The DSF values are in the 0-100% range. When the value is near to 0%, it represents less or no similarity between the segmented and ground truth regions. If the DSF value is near 100%, then the segmented and ground truth regions are similar. The DSF for proposed model and state-of-art is shown in *Figure 7*.

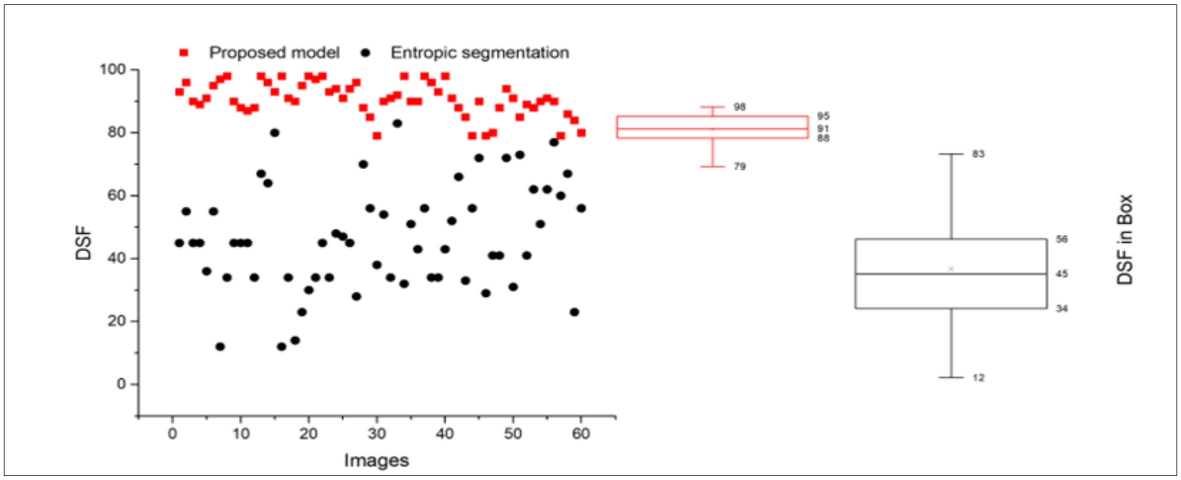

Figure 7 Performance comparison of the proposed model with entropic technique using DSF

5.Discussion

In this section, the efficiency of the proposed framework is compared with threshold segmentation using minimum cross entropy. *Figure 8* shows a comparison of proposed model with threshold segmentation using minimum cross entropy. In *Figure 8*, column (a) shows the CT scan images; column (b) illustrates the segmentation results of threshold segmentation using minimum cross entropy; column (c) illustrates the result of the proposed model; column (d) illustrates the ground truth images.

The availability of sophisticated tools for capturing high-quality images has also resulted in a considerable increase in the data volume. This requires the segmentation of the 'Region of Interest' (ROI) in the image for quicker analysis and better diagnosis. Furthermore, segmentation removes unwanted features from a scan, such as air, and separates the object from bone and neighbouring organs. This forms the basis for analytical interpretation and the selection of diagnostic methods. A highly precise biomedical segmentation technique is a primary goal, as it significantly impacts outcomes such as tracking the progression of tumors and assessing the effects of medication.

Numerous segmentation algorithms have been proposed by researchers based on edges, pixel intensity, shape, size, color, texture, entropy, and other factors. Among all types of segmentation algorithms, threshold-based segmentation techniques are the least time-consuming and have lower computational complexity.

The liver is associated with more than 100 diseases, majorly cirrhosis, fatty liver, cancer and other diseases. These diseases change the pixel intensity, texture, size, shape and colour of the liver. Hence, most of the liver segmentation algorithms fail to obtain precise results.

In the field of liver healthcare, doctors need to examine a voluminous number of images generated by imaging modalities such as CT, MRI, and PET. This makes the analysis and prediction of liver diseases difficult within a short time frame. Liver segmentation techniques are crucial for the success of the system, as precise segmentation enables better exploration and more accurate diagnosis.

Entropy is used in the quantitative exploration and estimation of image details. Its significance lies in its ability to provide important information about the image. Entropy in an image measures the amount of information that can be extracted from it. In the proposed framework, the entropy characteristics of the liver are studied in detail by randomly cropping sections of the liver and then calculating the entropy of the liver image. This provides accurate threshold values, which, in turn, result in the accurate delineation of the liver from abdominal CT scan images using the proposed segmentation framework. The average RVD, MED, accuracy and DSF are 12.5%, 4.2 mm, 91.7%, and 90.95%, respectively. *Table 1* compares the average values of RVD, MED, accuracy, and DSF of the proposed model with those of the minimum cross-entropy-based liver segmentation.

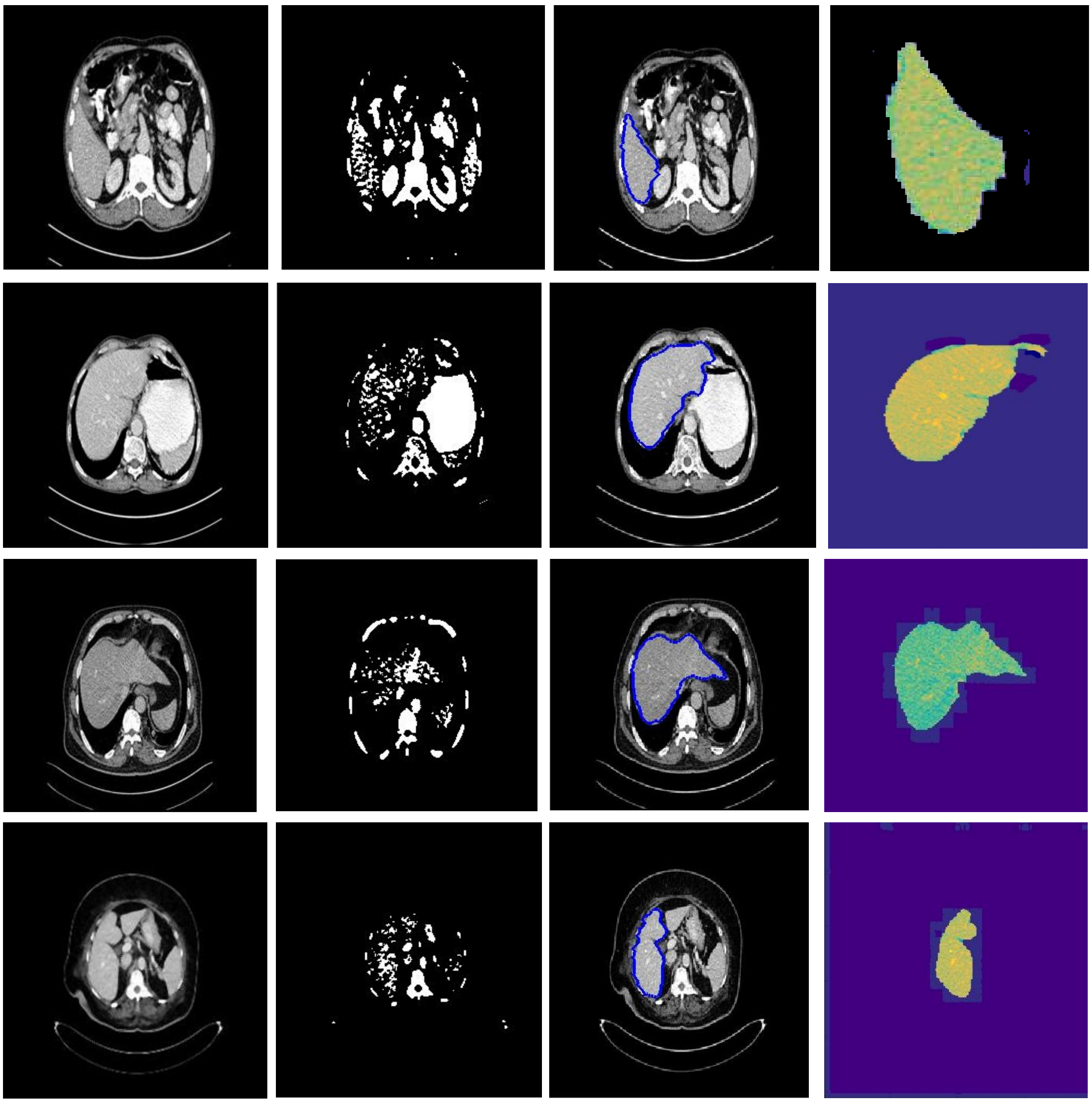

(a) (b) (c) (d)

Figure 8 Comparison of entropic liver segmentation model with state-of-art; column (a) illustrates the 2D-CT scan images; (b) Outcome of threshold segmentation using minimum cross entropy; (c) Outcome of proposed model; (d) Ground truth images

Table 1 Comparison of average RVD, MED, accuracy and DSF for proposed model and threshold segmentation using minimum cross entropy

Method	Average RVD in %	Average MED in mm	Average accuracy in %	Average DSF in %
Threshold segmentation using minimum cross entropy	56.2	48.4	70.23	47.11
Proposed model	12.5	4.2	91.7	90.95

Overall, the proposed liver segmentation model significantly benefits surgical planning, biological research, and disease diagnosis. By improving diagnostic accuracy and enhancing research capabilities, this method contributes to better patient care and more effective management of liver diseases. Clinicians can evaluate treatment responses and adapt therapeutic strategies based on quantitative measurements of changes in lesion size or liver volume. The upper bound and lower bound for threshold-based segmentation are determined by cropping a random section of the liver image. If a disease is not included in the randomly cropped section, the upper and lower bounds may not be optimal. This may lead to over- segmentation or under-segmentation. If cancer cells are present at the liver's border, the proposed model may fail to accurately identify the liver in an abdominal CT scan image. One of the key difficulties with our approaches is intensity inhomogeneity inside the liver tissue. The liver frequently shows varied intensities due to diverse tissue types and pathological alterations, making it challenging to create thresholds that reliably distinguishes liver tissue from surrounding organs and structures. The liver's unusual shape complicates thresholding procedures. A complete list of abbreviations is listed in *Appendix I*.

6.Conclusion and future work

Many algorithms have been designed for automatic selection of precise threshold values. One class of selection schemes is based on the principle of entropy, or the information randomness of an image, and is known as the entropic threshold method. Entropy is one of the most effective methods for extracting information content from an image. In this paper, the entropy distribution of the liver section is split into two sub-distributions, which maximize the entropy of each range: (1) foreground distribution and (2) background distribution. The foreground distribution is analyzed to determine the lower bound and the upper bound. These bounds are then used to demarcate the liver in CT scan images. This approach is highly effective and provides precise threshold values which are the backbone for success of a threshold-based liver segmentation. The results show significant improvements in the performance of the proposed model. This concept can also be applied to segment other organs, such as kidneys, spleen, gallbladder, etc., and can be used to separate tumors associated with these organs. Through the analysis of the entropy distribution, the technique establishes lower and upper boundaries that function as useful thresholds for defining liver tissue, improving segmentation accuracy. Comparing the suggested model to conventional techniques, the segmentation performance shows notable gains. Its capacity to adaptively choose threshold values according to the particulars of the liver segment under analysis is responsible for this. In addition to the liver, additional organs like the kidneys, spleen, and gallbladder can also be segmented using the same entropic threshold-based principles. It may also be useful in detecting cancers connected to these components. An important development in automated liver segmentation is this entropic thresholding method, which offers a strong foundation that may be modified for more extensive uses in medical imaging.

The shortcomings of proposed methods—intensity inhomogeneity, poor boundary detection, noise sensitivity, anatomical variability, liver geometry complexity, and reliance on user input—highlight the need for more sophisticated approaches even though they offer a simple method for liver segmentation. In liver segmentation tasks, hybrid approaches that integrate thresholding with machine learning or deep learning techniques may provide increased accuracy and resilience. By offering precise volumetric measures, segmentation techniques may help with liver transplantation planning and tumor assessment as their use in clinical settings grows.

Acknowledgment

None.

Conflicts of interest

The authors have no conflicts of interest to declare.

Data availability

The test dataset comprises CT scans of 60 different patients which are collected from CT scan Centre, LG F, Eureka

Junction, 6-13, Travellers Bunglow Rd, Deshpande Nagar, Hubballi, Karnataka 580029, India. This data is available on request from the corresponding author upon reasonable request.

Author's contribution statement

Sangeeta K Siri: Conceptualization, design, study conception, implementation, interpretation of results and writing original draft. **Sudha M S:** Data acquisition, data collection, Writing – review and editing. **Baby H T:** Data curation, data analysis, Writing – review and editing. **Pramod Kumar S:** Interpretation of results, supervision, investigation on challenges, Writing – review and editing. **Pradeepa S C:** Interpretation of results and proof reading. **Abhijith N:** Writing – review and editing.

References

[1] Castell DO, O'brien KD, Muench H, Chalmers TC. Estimation of liver size by percussion in normal individuals. Annals of Internal Medicine. 1969; 70(6):1183-9.

[2] Tortora GJ, Derrickson BH. Principles of anatomy and physiology. John Wiley & Sons; 2018.

[3] Osna NA, Donohue JTM, Kharbanda KK. Alcoholic liver disease: pathogenesis and current management. Alcohol Research: Current Reviews. 2017; 38(2):147-61.

[4] Campadelli P, Casiraghi E, Esposito A. Liver segmentation from computed tomography scans: a survey and a new algorithm. Artificial Intelligence in Medicine. 2009; 45(2-3):185-96.

[5] Bray F, Ferlay J, Soerjomataram I, Siegel RL, Torre LA, Jemal A. Global cancer statistics: GLOBOCAN estimates of incidence and mortality worldwide for 36 cancers in 185 countries. CA: A Cancer Journal for Clinicians. 2018; 68(6):394-424.

[6] Oh JH, Jun DW. The latest global burden of liver cancer: a past and present threat. Clinical and Molecular Hepatology. 2023; 29(2):355-7.

[7] Varghese AP, Naik S, Andrabi SA, Luharia A, Tivaskar S. Enhancing radiological diagnosis: a comprehensive review of image quality assessment and optimization strategies. Cureus. 2024; 16(6):1-10.

[8] Lim SJ, Jeong YY, Ho YS. Automatic liver segmentation for volume measurement in CT images. Journal of Visual Communication and Image Representation. 2006; 17(4):860-75.

[9] Lee CC, Chung PC, Chen YJ. Classification of liver diseases from CT images using BP-CMAC neural network. In 9th international workshop on cellular neural networks and their applications 2005 (pp. 118-21). IEEE.

[10] Gletsos M, Mougiakakou SG, Matsopoulos GK, Nikita KS, Nikita AS, Kelekis D. A computer-aided diagnostic system to characterize CT focal liver lesions: design and optimization of a neural network classifier. IEEE Transactions on Information Technology in Biomedicine. 2003; 7(3):153-62.

[11] Zhou X, Kitagawa T, Okuo K, Hara T, Fujita H, Yokoyama R, et al. Construction of a probabilistic atlas for automated liver segmentation in non-contrast torso CT images. In international congress series 2005 (pp. 1169-74). Elsevier.

[12] Di S, Zhao Y, Liao M, Yang Z, Zeng Y. Automatic liver tumor segmentation from CT images using hierarchical iterative superpixels and local statistical features. Expert Systems with Applications. 2022; 203(C):117347.

[13] Oliver3rd JH, Baron RL. Helical biphasic contrast-enhanced CT of the liver: technique, indications, interpretation, and pitfalls. Radiology. 1996; 201(1):1-4.

[14] Zareei A, Karimi A. Liver segmentation with new supervised method to create initial curve for active contour. Computers in Biology and Medicine. 2016; 75:139-50.

[15] Shu X, Yang Y, Wu B. Adaptive segmentation model for liver CT images based on neural network and level set method. Neurocomputing. 2021; 453:438-52.

[16] He R, Xu S, Liu Y, Li Q, Liu Y, Zhao N, et al. Three-dimensional liver image segmentation using generative adversarial networks based on feature restoration. Frontiers in Medicine. 2022; 8:1-17.

[17] Gotra A, Sivakumaran L, Chartrand G, Vu KN, Vandenbroucke-MF, Kauffmann C, et al. Liver segmentation: indications, techniques and future directions. Insights Into Imaging. 2017; 8:377-92.

[18] Jiang H, Li S, Li S. Registration-based organ positioning and joint segmentation method for liver and tumor segmentation. BioMed Research International. 2018; 2018(1):1-11.

[19] Yang W, Cai L, Wu F. Image segmentation based on gray level and local relative entropy two dimensional histogram. Plos One. 2020; 15(3):1-9.

[20] Lu X, Xie Q, Zha Y, Wang D. Fully automatic liver segmentation combining multi-dimensional graph cut with shape information in 3D CT images. Scientific Reports. 2018; 8(1):1-9.

[21] Nayantara PV, Kamath S, Kadavigere R, Manjunath KN. Automatic liver segmentation from multiphase CT using modified SegNet and ASPP module. SN Computer Science. 2024; 5(4):1-18.

[22] Ahmad M, Ding Y, Qadri SF, Yang J. Convolutional-neural-network-based feature extraction for liver segmentation from CT images. In Eleventh international conference on digital image processing 2019 (pp. 829-35). SPIE.

[23] Siri SK, Kumar SP, Vlatte M. Threshold-based new segmentation model to separate the liver from CT scan images. IETE Journal of Research. 2022; 68(6):4468-75.

[24] Siri SK, Latte MV. A novel approach to extract exact liver image boundary from abdominal CT scan using neutrosophic set and fast marching method. Journal of Intelligent Systems. 2019; 28(4):517-32.

[25] Zhang Z, Li G, Wang Z, Xia F, Zhao N, Nie H, et al. Deep-learning segmentation to select liver parenchyma for categorizing hepatic steatosis on multinational chest CT. Scientific Reports. 2024; 14(1):1-11.

[26] Alirr OI. Deep learning and level set approach for liver and tumor segmentation from CT scans. Journal of Applied Clinical Medical Physics. 2020; 21(10):200-9.
[27] Rahman H, Bukht TF, Imran A, Tariq J, Tu S, Alzahrani A. A deep learning approach for liver and tumor segmentation in CT images using ResUNet. Bioengineering. 2022; 9(8):1-19.
[28] Napte K, Mahajan A, Urooj S. ESP-UNet: encoder-decoder convolutional neural network with edge-enhanced features for liver segmentation. International Information and Engineering Technology Association. 2023; 40(5): 2275-81.
[29] Lou Q, Lin T, Qian Y, Lu F. Semi-supervised liver segmentation based on local regions self-supervision. Medical Physics. 2024; 51(5):3455-63.
[30] Gao Y, Guo J, Fu C, Wang Y, Cai S. VLSM-Net: a fusion architecture for CT image segmentation. Applied Sciences. 2023; 13(7):1-12.
[31] Özcan F, Uçan ON, Karaçam S, Tunçman D. Fully automatic liver and tumor segmentation from CT image using an AIM-Unet. Bioengineering. 2023; 10(2):1-21.
[32] Ayalew YA, Fante KA, Mohammed MA. Modified U-Net for liver cancer segmentation from computed tomography images with a new class balancing method. BMC Biomedical Engineering. 2021; 3:1-13.
[33] Khoshkhabar M, Meshgini S, Afrouzian R, Danishvar S. Automatic liver tumor segmentation from CT images using graph convolutional network. Sensors. 2023; 23(17):1-21.
[34] Balakrishnan P, Baskaran B, Vivekanandan S, Gokul P, Sathiya B. Liver segmentation using Mnet for cirrhosis. Measurement: Sensors. 2024; 31:100986.
[35] Giri J, Sathish T, Sheikh T, Sunheriya N, Giri P, Chadge R, et al. Automatic liver segmentation using U-Net deep learning architecture for additive manufacturing. Interactions. 2024; 245(1):1-11.
[36] Uplaonkar DS, Virupakshappa, Patil N. Modified Otsu thresholding based level set and local directional ternary pattern technique for liver tumor segmentation. International Journal of System Assurance Engineering and Management. 2024; 15(1):73-83.
[37] Cao G, Sun Z, Wang C, Geng H, Fu H, Yin Z, et al. RASNet: renal automatic segmentation using an improved U-Net with multi-scale perception and attention unit. Pattern Recognition. 2024; 150:110336.
[38] Ouyang S, He B, Luo H, Jia F. SwinD-Net: a lightweight segmentation network for laparoscopic liver segmentation. Computer Assisted Surgery. 2024; 29(1):1-9.
[39] Biswas A, Maity SP, Banik R, Bhattacharya P, Debbarma J. GAN-driven liver tumor segmentation: enhancing accuracy in biomedical imaging. SN Computer Science. 2024; 5:652.
[40] Shannon CE. A mathematical theory of communication. The Bell System Technical Journal. 1948; 27(3):379-423.
[41] Seising R. 60 years" a mathematical theory of communication"-towards a" fuzzy information theory". In IFSA/EUSFLAT conference 2009 (pp. 1332-7).
[42] Hinojosa S, Dhal KG, Abd EM, Oliva D, Cuevas E. Entropy-based imagery segmentation for breast histology using the stochastic fractal search. Neurocomputing. 2018; 321:201-15.
[43] Mello RJC, Vazquez NJL, Legal-ayala H, Pinto-roa DP, Gomez-guerrero S, García TM. Entropy and contrast enhancement of infrared thermal images using the multiscale top-hat transform. Entropy. 2019; 21(3):1-19.
[44] Saraiva P. On Shannon entropy and its applications. Kuwait Journal of Science. 2023; 50(3):194-9.
[45] Tsai DY, Lee Y, Matsuyama E. Information entropy measure for evaluation of image quality. Journal of Digital Imaging. 2008; 21:338-47.
[46] Eiseman NA, Bianchi MT, Westover MB. The information theoretic perspective on medical diagnostic inference. Hospital Practice. 2014; 42(2):125-38.
[47] Udupa JK, Leblanc VR, Zhuge Y, Imielinska C, Schmidt H, Currie LM, et al. A framework for evaluating image segmentation algorithms. Computerized Medical Imaging and Graphics. 2006; 30(2):75-87.
[48] Zhu Y, Wei R, Gao G, Ding L, Zhang X, Wang X, et al. Fully automatic segmentation on prostate MR images based on cascaded fully convolution network. Journal of Magnetic Resonance Imaging. 2019; 49(4):1149-56.
[49] Taha AA, Hanbury A. Metrics for evaluating 3D medical image segmentation: analysis, selection, and tool. BMC Medical Imaging. 2015; 15:1-28.
[50] Min J, Powell M, Bowyer KW. Automated performance evaluation of range image segmentation algorithms. IEEE Transactions on Systems, Man, and Cybernetics, Part B (Cybernetics). 2004; 34(1):263-71.
[51] Heimann T, Van GB, Styner MA, Arzhaeva Y, Aurich V, Bauer C, et al. Comparison and evaluation of methods for liver segmentation from CT datasets. IEEE Transactions on Medical Imaging. 2009; 28(8):1251-65.
[52] Wang Z. Monitoring of GMAW weld pool from the reflected laser lines for real-time control. IEEE Transactions on Industrial Informatics. 2014; 10(4):2073-83.

Sangeeta K Siri completed her Bachelor of Engineering degree in 1998 from SDMCET, Dharwad, Karnataka, India. She earned her Master's degree in Electronics from BMSCE, Bangalore, Karnataka, India, and was awarded a Ph.D. from VTU, Belagavi, Karnataka, India. She is currently working as a Professor in the Electronics and Communication Department at Global Academy of Technology (GAT),

Bengaluru, Karnataka, India. Her areas of interest include Image Processing and Pattern Recognition.
Email: sangeeta_mk@rediffmail.com

Sudha M S has over 25 years of teaching experience and currently serves as an Associate Professor at the Cambridge Institute of Technology. She is a member of IEEE in the Circuits and Systems Society. She has published research articles in various indexed journals and has attended and presented papers at IEEE conferences. Additionally, she has filed and published several patents for innovative work conducted in collaboration with her students.
Email: sudharajoli94@gmail.com

Baby H T is an Associate Professor at Government Engineering College, Mosalehosahalli, Hassan, with 21 years of teaching experience in various esteemed organizations. She completed her M.Tech in Digital Communication and Networking from SJCIT, Chickballapur, in 2005 and earned her Ph.D. from VTU University in 2021. Her areas of interest include Cryptography, Information Theory and Coding, Network Security, and Image Processing. She has published research papers in numerous international and national conferences and journals.
Email: babygowda@gmail.com

Pramod Kumar S received his B.E. degree in Electronics and Communication Engineering from VEC, Bellary, and his M.Tech in VLSI Design and Embedded Systems from UTL Technologies Limited, Bangalore. He was awarded a Ph.D. from VTU-RRC, Belgaum, and is currently serving as a faculty member in the Electronics and Communication Engineering Department at JNN College of Engineering, Shivamogga, Karnataka, India.
Email: pramod.s86@gmail.com

Pradeepa S C is currently working as an Assistant Professor in the Electronics and Communication Department at JNN College of Engineering, Shivamogga, Karnataka. He has 12 years of teaching experience, and his areas of interest include VLSI Design, Embedded Systems, and Microcontroller Programming. He is currently pursuing Ph.D. in the field of Wireless Sensor Networks.
Email: pradeepasc@jnnce.ac.in

Abhijith N is currently working as an Assistant Professor in the Electronics and Communication Department at JNN College of Engineering, Shivamogga, Karnataka. He has 14 years of teaching experience, and his areas of interest include Image Processing, VLSI Design, Embedded Systems, and Microcontroller Programming. He is currently pursuing Ph.D. in the field of Wireless Sensor Networks.
Email: abhijithn@jnnce.ac.in

Appendix I

S. No.	Abbreviation	Description
1	3D	Three Dimensions
2	CAD	Computer-Aided Disease
3	CNN	Convolutional-Neural Network
4	CT	Computed Tomography
5	DC	Dice Score
6	DSF	Dice Similarity Factor
7	FCN	Fully Convolutional Neural Network
8	GAN	Generative Adversarial Network
9	GPU	Graphics Processing Unit
10	HGA	Hybrid Genetic Algorithm
11	IoU	Intersection of Union
12	IRCAD	Research Institute Against Digestive Cancer
13	JC	Jaccard Coefficient
14	LiTS	Liver Tumor Segmentation Benchmark
15	MED	Maximum Edge Distance
16	MRI	Magnetic Resonance Imaging
17	PET	Positron Emission Tomography
18	ReLU	Rectified Linear Unit
19	ResNet	Residual Network
20	ResUNet	Residual U-Net
21	RVD	Relative Volume Difference
22	SDD	Slope Difference Distribution
23	SegNet	Segmented Neural Network